Acoustic modal expansion of open cavity using coupled mode theory

Yuhui Tong, Yiwei Kou, Jie Pan*

Schoold of Mechanical and Chemical Engineering, The University of Western Australia, Crawley, WA 6009, Australia

Abstract

The modal description of closed acoustical systems such as rooms and enclosure is well known and is commonly used to find the forced response at a given frequency as the superposition of the eigenmodes. Not much literature, however, exists on calculating the forced reponse using the modal description of sound radiated from open cavities, despite their significant practical importance. Taking a baffled rectangular open cavity as an example, it is provided in the present paper a solid theoretical formulation and corresponding numerical verification to show that, the forced response of such an open cavity system can be expressed via superposition of bi-orthogonal frequency-dependent eigenmodes.

*Author to whom correspondence should be addressed.
Email: jie.pan@uwa.edu.au

1 Introduction

Open acoustic cavities are common structures in the context of wheel wells of aircrafts, sound barriers, and etc. The eigenmodes of acoustic resonance of the open cavity were investigated intensively for the benifits of passive and active noise control [3, 1]. It is noted, however, there has long been an abscence of literature that successfully dealt with the calculation of the forced response using the eigen-modal description of sound radiated from open cavities. The challenge lies in the non-orthogonality and incompleteness of eigenmodes defined by the acoustic resonance, as implicitly or explicitly stated in Refs. [5, 2, 11]. For example, Yang, et al., [11], predicted the transmission loss of a noise barrier by expanding sound field into eigenmodes solved numerically using perfectly matched layers (PMLs), but found predictions reliable only at frequencies close to eigenvalues and inaccurate elsewhere.

Progresses were reported in a related problem regarding the scattering in acoustic scatterers that coupled mode theory were employed to include the coupling between cavity and rigid ducts[7, 10]. It is then demostrated that the scattered field can be expressed as the superposition of a set of frequency-dependent eigenmodes [Tong, Pan, 2016, arXiv]. In the present paper, the approach in Ref. [Tong, Pan, 2016, arXiv] is extened to open cavity problem where a baffled rectangular open cavity with sound source placed inside the cavity is considered. The eigen value problem is derived at a given frequency for the definition of the corresponding frequency-dependent eigenmodes (not the eigenmode of acoustic resonance), giving rise to the modal expansion of sound field inside and outside the cavity in terms of these eigenmodes. Numerical study is also presented and discussed to examine the effectiveness

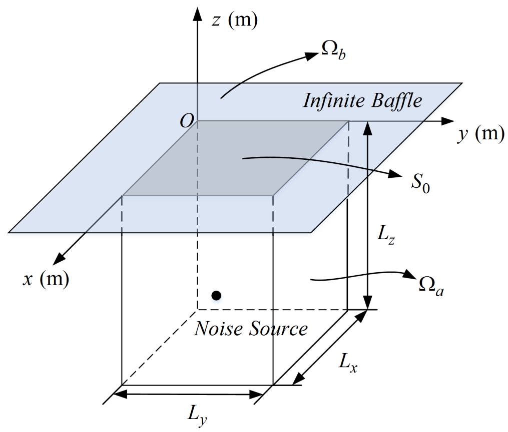

Figure 1: A schematic diaggram of an baffled open cavity.

as well as the accuracy of the proposed method.

2 Theory

2.1 Phase I, problem formulation

As depicted in Fig. 1, the rectangular cavity with an opening located at an infinite baffle is investigated in the present paper. For the sake of simplicity, all boundaries are assumed to be rigid.

The sound pressure (omitting the time dependence $e^{j\omega t}$) excited by a monopole source inside the cavity can be obtained by solving the inhomogeneous Helmholtz equation

$$\nabla^2 p + k^2 p = -q_s \delta(\boldsymbol{x} - \boldsymbol{x}_s), \tag{1}$$

where $k = \omega/c_0$ is the wavenumber, c_0 is the speed of sound, q_s is the source strength, $\boldsymbol{x}_s$ is the position of the monopole source, which is supposed to be within the cavity. The solution of Eq. (1) can be written respectively for the volume occupied by the cavity Ω_a, and upper half space Ω_b. For Ω_a,

$$p_a(\boldsymbol{x}) = \sum_{\mu,\nu,\xi} a_{\mu,\nu,\xi}\phi_{\mu,\nu,\xi}(\boldsymbol{x}), \tag{2}$$

where $\phi_{\mu',\nu',\xi'}(\boldsymbol{x}) = \psi_{\mu'}(x)\psi_{\nu'}(y)\psi_{\xi'}(z)$ is the eigenmode for *enclosed* cavity and $\psi_m(x) = \sqrt{\frac{2-\delta_{0,m}}{L_x}}\cos(\frac{m\pi}{L_x}x)$. For Ω_b,

$$p_b(\boldsymbol{x}) = jk\rho_0 c_0 \iint_{S_0} G_b(\boldsymbol{x}, \boldsymbol{x}')v_\perp(\boldsymbol{x}')dS', \tag{3}$$

where $G_b(\boldsymbol{x}, \boldsymbol{x}') = \frac{1}{2\pi}\frac{e^{-jk|\boldsymbol{x}-\boldsymbol{x}'|}}{|\boldsymbol{x}-\boldsymbol{x}'|}$ is the Green's function for the upper half space, ρ_0 is the ambient air density, $v_\perp(\boldsymbol{x}')$ is the normal velocity distribution at the opening S_0 (the intersection between Ω_a and Ω_b), the integral is invaluated over S_0.

In Ω_a, p_a satisfies,

$$\nabla^2 p_a(\boldsymbol{x}) + k^2 p_a(\boldsymbol{x}) = -q_s\delta(\boldsymbol{x} - \boldsymbol{x}_s), \tag{4}$$

together with corresponding boundary conditions, while $\phi_{\mu,\nu,\xi}$ satisfies,

$$\nabla^2\phi_{\mu,\nu,\xi} + k^2_{\mu,\nu,\xi}\phi_{\mu,\nu,\xi} = 0, \tag{5}$$

$$k^2_{\mu,\nu,\xi} = (\mu\pi/L_x)^2 + (\nu\pi/L_y)^2 + (\xi\pi/L_z)^2,$$

and rigid boundary condition for all six walls of the rectangular cavity, including S_0. Multiplying Eq. (4) and Eq. (5) by $\phi_{\mu,\nu,\xi}$ and p_a respectively and taking the difference of the resulting equations yields,

$$\left(p_a\nabla^2\phi_{\mu,\nu,\xi} - \phi_{\mu,\nu,\xi}\nabla^2 p_a\right) + (k^2_{\mu,\nu,\xi} - k^2)p_a\phi_{\mu,\nu,\xi} = q_s\phi_{\mu,\nu,\xi}\delta(\boldsymbol{x} - \boldsymbol{x}_s). \tag{6}$$

Integrating over Ω_a and applying Green's theorem gives

$$jk\rho_0 c_0 \iint_{S_0} \phi_{\mu,\nu,\xi} v_\perp dS_0 + (k^2_{\mu,\nu,\xi} - k^2) a_{\mu,\nu,\xi} = q_0 \phi_{\mu,\nu,\xi}(\boldsymbol{x}_s). \tag{7}$$

The above equation can be further simplied into

$$\sum_{m,n} jk\psi_\xi(0)\delta_{\mu,m}\delta_{\nu,n}\rho_0 c_0 V_{m,n} + (k^2_{\mu,\nu,\xi} - k^2) a_{\mu,\nu,\xi} = q_0 \phi_{\mu,\nu,\xi}(\boldsymbol{x}_s), \tag{8}$$

by using the expansion of $v_\perp(x, y)$

$$v_\perp(x, y) = \sum_{m,n} V_{m,n} \psi_m(x) \psi_n(y). \tag{9}$$

Another constraint is the continuity condition for sound pressure at the interface, i.e., $p_a|_{S_0} = p_b|_{S_0}$ such that

$$\sum_{\mu',\nu',\xi'} a_{\mu',\nu',\xi'} \psi_{\mu'}(x)\psi_{\nu'}(y)\psi_{\xi'}(0) = jk\rho_0 c_0 \iint_{S_0} \frac{e^{-jk\sqrt{(x-x')^2+(x-y')^2}}}{2\pi\sqrt{(x-x')^2+(x-y')^2}} \sum_{m,n} V_{m,n}\psi_m(x')\psi_n(y') dS_0 \tag{10}$$

Multiplying $\psi_\mu(x)\psi_\nu(y)$ and integrate over the interface leads to,

$$\sum_{\mu',\nu',\xi'} \delta_{\mu,\mu'}\delta_{\nu,\nu'}\psi_{\xi'}(0) a_{\mu',\nu',\xi'} = \rho_0 c_0 \sum_{m,n} Z_{\mu,\nu,m,n} V_{m,n}, \tag{11}$$

where $Z_{\mu,\nu,m,n}$ is the radiation impedance of an baffled rectangular plate [6] of $L_x \times L_y$

$$Z_{\mu,\nu,m,n} = jk \iint_{S_0} \iint_{S_0} \psi_\mu(x)\psi_\nu(y) \frac{e^{-jk\sqrt{(x-x')^2+(x-y')^2}}}{2\pi\sqrt{(x-x')^2+(x-y')^2}} \psi_m(x')\psi_n(y') dS' dS \tag{12}$$

Using Eqs. (8) and (11), vectors $\boldsymbol{a} = \begin{bmatrix} \cdots & a_{\mu,\nu,\xi} & \cdots \end{bmatrix}^T$ and $\boldsymbol{V} = \begin{bmatrix} \cdots & V_{m,n} & \cdots \end{bmatrix}^T$ can be determined by solving

$$\boldsymbol{HV} + (\boldsymbol{K} - k^2\boldsymbol{I})\boldsymbol{a} = \boldsymbol{S} \tag{13}$$

$$\boldsymbol{Ma} = \boldsymbol{ZV} \tag{14}$$

where corresponding matrices are defined as follows: $\boldsymbol{H}_{(\mu,\nu,\xi),(m,n)} = jk\delta_{\mu,m}\delta_{\nu,n}\psi_\xi(0)$, $\boldsymbol{K}_{(\mu,\nu,\xi),(\mu',\nu',\xi')} = k^2_{\mu,\nu,\xi}\delta_{\mu,\mu'}\delta_{\nu,\nu'}\delta_{\xi,\xi'}$, $\boldsymbol{S} = q_s \begin{bmatrix} \cdots & \phi_{\mu,\nu,\xi}(\boldsymbol{x}_s) & \cdots \end{bmatrix}^T$, $\boldsymbol{M}_{(m,n),(\mu,\nu,\xi)} = \delta_{\mu,\mu'}\delta_{\nu,\nu'}\psi_{\xi'}(0)$, $\boldsymbol{Z}_{(\mu,\nu),(m,n)} = Z_{\mu,\nu,m,n}$. Eqs. (13) and (14) can be further reduced to

$$(\boldsymbol{D} - \boldsymbol{k^2})\boldsymbol{a} = \boldsymbol{S}, \tag{15}$$

where $\boldsymbol{D} = \boldsymbol{K} - \boldsymbol{HZ}^{-1}\boldsymbol{M}$ is known as effective Hamiltonian (reduced differential operator) in quantum physics [8].

2.2 Phase II Bi-orthogonal basis and modal expansion.

Eq. (15) gives rise to the following eigenvalue problem

$$\boldsymbol{Dg}_{\mu,\nu,\xi} = K^2_{\mu,\nu,\xi}\boldsymbol{g}_{\mu,\nu,\xi}, \tag{16}$$

where $K^2_{\mu,\nu,\xi}$ is the eigenvalue and the eigenvector $\boldsymbol{g}_{\mu,\nu,\xi}$ satisfies the bi-orthogonal relation [Tong, Pan, arXiv]

$$\boldsymbol{g}^T_{\mu',\nu',\xi'}\boldsymbol{g}_{\mu,\nu,\xi} = \delta_{\mu',\mu}\delta_{\nu,\nu'}\delta_{\xi,\xi'}\boldsymbol{g}^T_{\mu,\nu,\xi}\boldsymbol{g}_{\mu,\nu,\xi}. \tag{17}$$

An alternative expression of Eq. (17) is written as,

$$\iiint_{V_0} \Phi_{\mu',\nu',\xi'}(\boldsymbol{x})\Phi_{\mu,\nu,\xi}(\boldsymbol{x})dV = \delta_{\mu',\mu}\delta_{\nu,\nu'}\delta_{\xi,\xi'} \iiint_{V_0} \Phi^2_{\mu,\nu,\xi}(\boldsymbol{x})dV, \tag{18}$$

where $\Phi_{\mu,\nu,\xi}(\boldsymbol{x})$ is the modal function corresponding to $\boldsymbol{g}_{\mu,\nu,\xi}$ such that

$$\Phi_{\mu,\nu,\xi}(\boldsymbol{x}) = \sum_{\mu',\nu',\xi'} \left(\boldsymbol{g}_{\mu,\nu,\xi}\right)_{\mu',\nu',\xi'} \phi_{\mu',\nu',\xi'}(\boldsymbol{x}). \tag{19}$$

Expanding $\boldsymbol{a}$ into $\left\{\boldsymbol{g}_{\mu,\nu,\xi}\right\}$

$$\boldsymbol{a} = \sum_{\mu',\nu',\xi'} c_{\mu',\nu',\xi'}\boldsymbol{g}_{\mu',\nu',\xi'} \tag{20}$$

and making the substitution into Eq. (15) yields

$$c_{\mu,\nu,\xi} = \frac{\boldsymbol{g}^T_{\mu,\nu,\xi}\boldsymbol{S}}{(K^2_{\mu,\nu,\xi} - k^2)\boldsymbol{g}^T_{\mu,\nu,\xi}\boldsymbol{g}_{\mu,\nu,\xi}}. \tag{21}$$

Combining Eq. (20) together with Eqs. (2 ,3,14) leads to the modal expansion of sound pressure of the open cavity,

$$p(\boldsymbol{x}) = \begin{pmatrix} p_a(\boldsymbol{x}) \\ p_b(\boldsymbol{x}) \end{pmatrix} = \sum_{\mu,\nu,\xi} c_{\mu,\nu,\xi} \begin{pmatrix} \Phi_{\mu,\nu,\xi}(\boldsymbol{x}) \\ \Psi_{\mu,\nu,\xi}(\boldsymbol{x}) \end{pmatrix}, \tag{22}$$

where $\Psi_{\mu,\nu,\xi}(\boldsymbol{x})$ is given by

$$\Psi_{\mu,\nu,\xi}(\boldsymbol{x}) = \boldsymbol{\varphi}^T\boldsymbol{Z}^{-1}\boldsymbol{M}\boldsymbol{g}_{\mu,\nu,\xi}. \tag{23}$$

Noted $\boldsymbol{\varphi} = \begin{bmatrix} \cdots & \varphi_{m,n}(\boldsymbol{x}) & \cdots \end{bmatrix}$, $\varphi_{m,n}(\boldsymbol{x}) = jk\rho_0 c_0 \iint_{S_0} G_b(\boldsymbol{x},\boldsymbol{x}')\psi_m(x')\psi_n(y')dS'$ is the sound pressure induced by velocity distribution $\psi_m(x')\psi_n(y')$ on S_0.

μ	ν	ξ	$f_{\mu,\nu,\xi}$ (Hz)	$F_{\mu,\nu,\xi}$ (Hz)
0	0	0	0	133.26+23.55j
0	1	0	253.73	283.08+8.64j
0	0	1	284.28	382.88+71.04j
0	1	1	381.04	449.37+40.02j
1	0	0	393.51	413.08+3.68j
1	1	0	468.22	484.95+1.83j
1	0	1	485.46	544.96+20.79j
0	2	0	507.46	522.01+2.07j
1	1	1	547.77	603.52+11.06j
0	0	2	568.56	604.31+75.40j
0	2	1	581.66	631.25+11.13j
0	1	2	622.60	666.71+46.10j
1	2	0	642.16	655+0.40j
1	0	2	691.46	743.95+28.66j
1	2	1	702.03	752.1+3.30j

Table 1: The first 15 modes of closed and open rectangular cavity, and the corresponding frequencies. $f_{\mu,\nu,\xi} = k_{\mu,\nu,\xi}c_0/2\pi$ for closed cavity; $F_{\mu,\nu,\xi} = K_{\mu,\nu,\xi}c_0/2\pi$ for open cavity, at source frequency $f = 500Hz$.

3 Numerical validation

The theoretical results obtained in Sec. 2 is check numerically here. The cavity in Fig. 1 has the dimensions of 0.432m long (L_x), 0.67m wide (L_y) and 0.598m high (L_z), which was considered in Ref. [9]. The source is located at $(0.1,\ 0.1,\ -L_z + 0.1)$ m while the field points inside and outside the cavity are randomly chosen at $(0.2,\ 0.3,\ -L_z + 0.4)$ m and $(1.3,\ 1.4,\ -L_z + 1.5)$ m. The analytical method proposed in Sec. 2 is obtained with MATLAB codes, when 140 *closed* cavity modes are used for computation of eigensolutions to Eq. (16).

140 eigenmodes are obtained by analytical method for open rectangular cavity. Table. 1 lists the first 15 eigen solutions when noise frequency $f = 500$ Hz ($k = 9.24$), in constrast with the counterparts of closed cavity. It's clear that the eigenfrequencies of acoustic modes become complex in

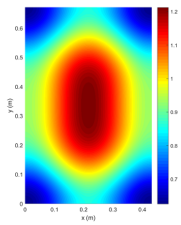
(0,0,0) mode $z = 0$ plane

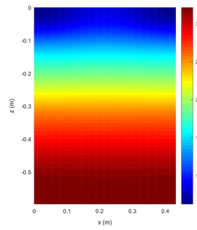
(0,0,0) mode $y = 0$ plane

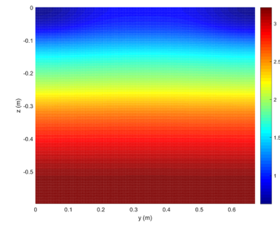
(0,0,0) mode $x = 0$ plane

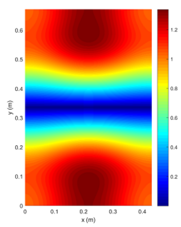
(0,1,0) mode $z = 0$ plane

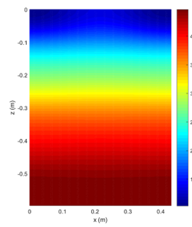
(0,1,0) mode $y = 0$ plane

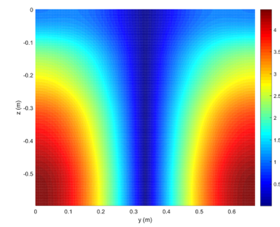
(0,1,0) mode $x = 0$ plane

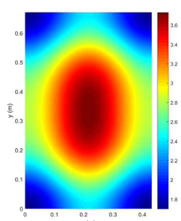
(0,0,1) mode $z = 0$ plane

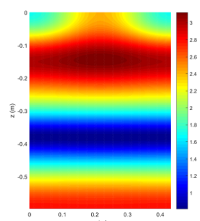
(0,0,1) mode $y = 0$ plane

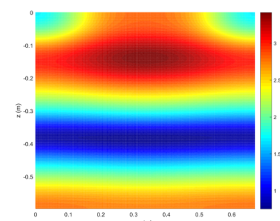
(0,0,1) mode $x = 0$ plane

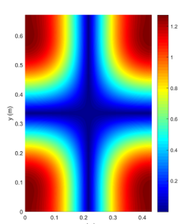
(1,1,0) mode $z = 0$ plane

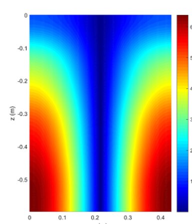
(1,1,0) mode $y = 0$ plane

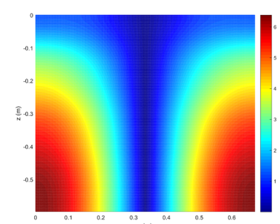
(1,1,0) mode $x = 0$ plane

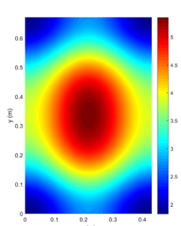
(0,0,2) mode $z = 0$ plane

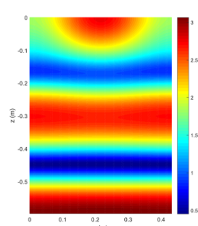
(0,0,2) mode $y = 0$ plane

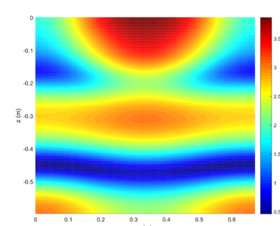
(0,0,2) mode $x = 0$ plane

Table 2: The modulus of $\Psi_{\mu,\nu,\xi}(\boldsymbol{x})$ for (0,0,0), (0,1,0), (0,0,1), (1,1,0), (0.0,2) modes, when source frequency $f = 500$ Hz.

$(\mu,\nu,\xi)\backslash(\mu',\nu',\xi')$	(0,0,0)	(0,1,0)	0,0,2)	(1,1,0)	(0,0,1)	(1,0,0)	(0,2,0)	(1,0,1)	(1,1,1)	(0,0,2)
(0,0,0)	0.9517	0	0	0	0	0	0	0	0	0
(0,1,0)	0	0.9717	0	0	0	0	0	0	0	0
0,0,2)	0	0	0.7803	0	0	0	0	0	0	0
(1,1,0)	0	0	0	0.9889	0	0	0	0	0	0
(0,0,1)	0	0	0	0	0.8956	0	0	0	0	0
(1,0,0)	0	0	0	0	0	0.9962	0	0	0	0
(0,2,0)	0	0	0	0	0	0	0.9890	0	0	0
(1,0,1)	0	0	0	0	0	0	0	0.9541	0	0
(1,1,1)	0	0	0	0	0	0	0	0	0.9835	0
(0,0,2)	0	0	0	0	0	0	0	0	0	0.7098

Table 3: $A_{(\mu,\nu,\xi),(\mu',\nu',\xi')}$ for first 10 eigenmodes, at source frequency $f = 500$ Hz. Noted in the table, values below 10^{-13} are taken as 0.

which the imaginary part corresponds to radiation loss. Table. 2 plots slices of $|\Psi_{\mu,\nu,\xi}|$, the modulus of modal function of (μ,ν,ξ) eigenmode. The nodal lines are distinguishable for these low frequency eigenmodes, which justifies the inheritance of the closed cavity modes' indexes μ,ν,ξ to classify the open cavity modes. The bi-orthogonality of the eigensolutions is validated in Tab. 3 by calculating

$$A_{(\mu,\nu,\xi),(\mu',\nu',\xi')} = |\boldsymbol{g}^T_{\mu,\nu,\xi}\boldsymbol{g}_{\mu,\nu,\xi}|, \tag{24}$$

where $\boldsymbol{g}_{\mu,\nu,\xi}$ is normalized such that $|\boldsymbol{g}^\dagger_{\mu,\nu,\xi}\boldsymbol{g}_{\mu,\nu,\xi}| = 1$. Figure. 3 presents the amplitude of each eigenmodes upon the monopole source with strength $q_s = jk\rho_0 c_0 q_0$, and $q_0 = 10^{-4} m^3/s$, where one can see that $|c_{\mu,\nu,\xi}|$ decays rapidly as the order of modes grows. $|c_{\mu,\nu,\xi}|$ takes the maximum value at (1,1,0) mode, of which the eigenfrequency takes $484.95 + 1.83j$ Hz. It is then examined the number of eigenmodes needed for calculation. Figure. 2 indicates less than 15 eigenmodes is necessary for sound pressure to converge at the probe points inside the cavity, while less than 20 eigenmodes for probe points outside the cavity. This result is quite reasonable considering the resonant eigenmode is the 6^{th} one.

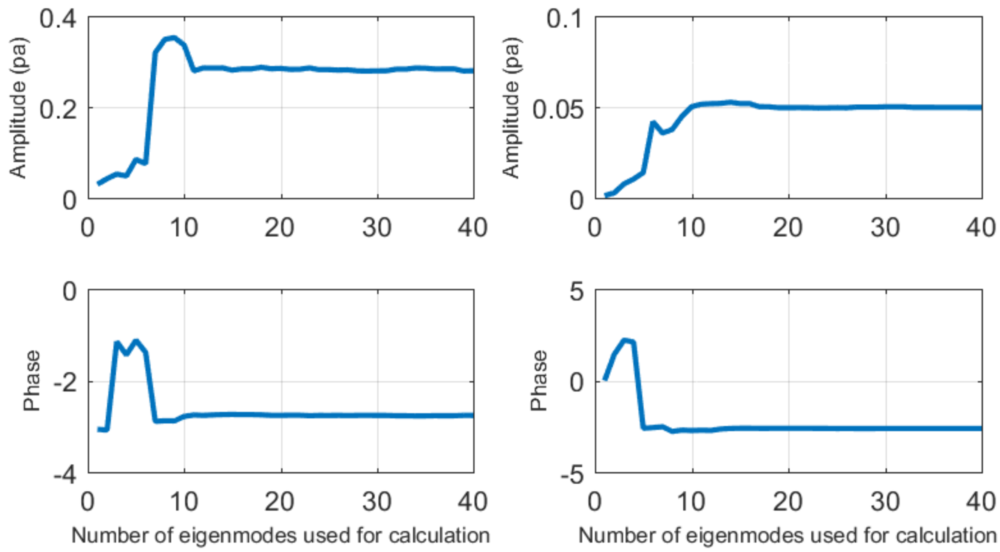

Figure 2: The calculated amplitude and phase of the sound pressure as a function of eigenmodes orders. The sound source is located at $(0.1,\ 0.1,\ -L_z+0.1)$ m with $f = 500Hz$, $q_s = 10^{-4}kg/s^2$; (left) location $(0.2,\ 0.3,\ -L_z{+}0.4)$ m in the cavity and (right) location $(1.3,\ 1.4,\ -L_z{+}1.5)$ m outside the cavity.

The performance of the proposed method is then verified by calculating the sound pressure at field points inside and outside cavity for multiple frequencies below 500 Hz, where calculation is implemented utilising 20 eigenmodes. The reference result is obtained via finite element software COMSOL, where PMLs are used to model the semi-infinite space above the baffle. Noted only frequencie above 30 Hz are treated in COMSOL, as at very low frequency, the PMLs needed for calculation become so thick to prevent reflected wave. The source strength is taken as $q_s = 4\pi \times 10^{-4}kg/s^2$ for all frequencies. Figure. 4 plots the comparison between results obtained by both methods, in which the excellent agreement verifies the effectiveness and accuracy of the proposed method.

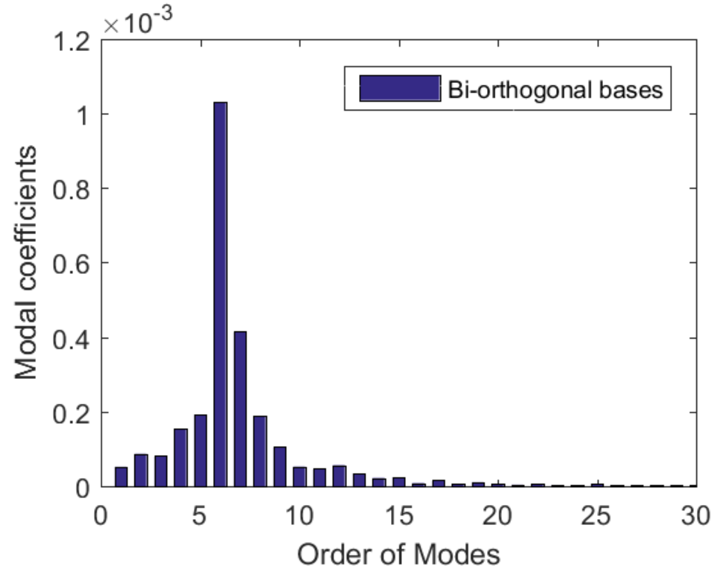

Figure 3: The amplitude of modal coefficients $|c_{\mu,\nu,\xi}|$, vs orders of mode, when source frequency is $500Hz$.

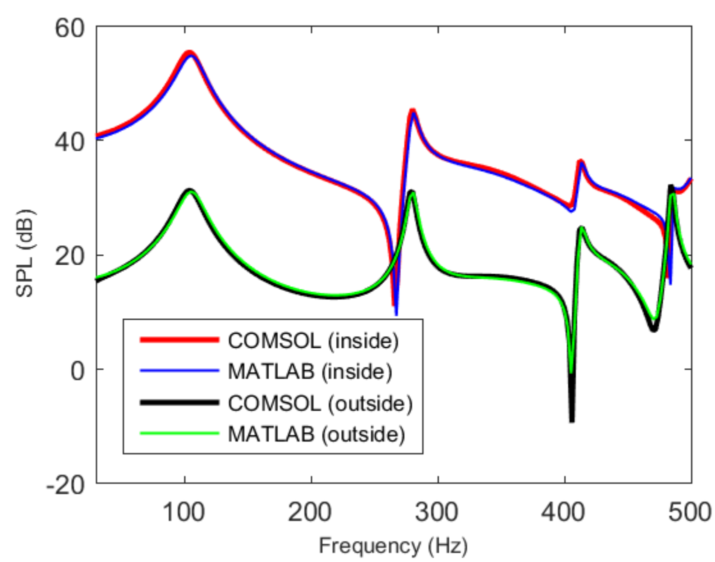

Figure 4: Comparison between the sound field obtained by the anlytical model (marked by MATLAB) and finite element simulation (marked by COMSOL) when the excitation point source is located at (0.1,0.1,0.1) m and $q_s = 4\pi \times 10^{-4} kg/s^2$; (a) sound pressure level at (0.2,0.3,0.4) m in the cavity and (1.3,1.4,1.5) m outside the cavity.

4 Conclusions and remarks

The acoustic forced response of a baffled rectangular open cavity at a given frequency has been formulated as the superposition of the bi-orthogonal frequency-dependent eigenmodes. The effectiveness of the proposed modal representation was demonstrated numerically by showing the accurate sound pressure prediction can be obtained using only a few eigenmodes for expansion, for field points either inside or outside the cavity. Noted the proposed method can be extended to baffled irregular open cavity straightforwardly by expanding the sound field inside the cavity with eigensolutions of the closed irregular cavity (corresponding to $\Psi_{\mu,\nu,\xi}(\boldsymbol{x})$ in the present paper), and that ouside the cavity with sound field radiated by baffled plate (corresponding to $\varphi_{m,n}(\boldsymbol{x})$). In the present paper, the source placed is placed inside the cavity; the case with source outside the cavity is technically solvable following the same step, but is more complex as the basis for external space, $\varphi_{m,n}(\boldsymbol{x})$ are non-orthogonal. The method may also be applicable to unbaffled open cavity, on condition that appropriate bases are found for internal and external spaces.

Finally, a remark is made on an eigenvalue problem similar to Eq. (16),

$$\boldsymbol{D}(\widetilde{K}^2_{\mu,\nu,\xi})\tilde{\boldsymbol{g}}_{\mu,\nu,\xi} = \widetilde{K}^2_{\mu,\nu,\xi}\tilde{\boldsymbol{g}}_{\mu,\nu,\xi}, \tag{25}$$

where the matrix $\boldsymbol{D}$ is eigenvalue dependent rather than k dependent. It corresponds to the natural vibration of the system in the absence of noise source, which is the *acoustic resonance* commonly encounted in literatures [3]. The Eq. (25) can be solved directly [10] and is equivalent to the solution by using the finite element eigen solver [4]. As mentioned in the introduction part, the eigensolutions to Eq. (25) are non-orthogonal and may not be complete for modal representation of the forced response of the system.

Acknowledgement

Authors wish to thank Shuping Wang from Nanjing University for discussion on the calculation of radiation impedance. Financial support from Australian Research Council (ARC LP) is gratefully acknowledged.

References

[1] Louis N Cattafesta, Qi Song, David R Williams, Clarence W Rowley, and Farrukh S Alvi. Active control of flow-induced cavity oscillations. *Progress in Aerospace Sciences*, 44(7):479–502, 2008.

[2] LM González, P Cobo, V Theofilis, and E Valero. Acoustic resonances in 2d open cavities. *Acta Acustica united with Acustica*, 99(4):572–581, 2013.

[3] Stefan Hein, Thorsten Hohage, and Werner Koch. On resonances in open systems. *Journal of Fluid Mechanics*, 506:255–284, 2004.

[4] Stefan Hein, Werner Koch, and Lothar Nannen. Trapped modes and fano resonances in two-dimensional acoustical duct–cavity systems. *Journal of fluid mechanics*, 692:257–287, 2012.

[5] James Leader and Jie Pan. On the completeness and orthogonality of the acoustic modes of an open cavity. In *Acoustics 2015 Hunter Valley*, 2015.

[6] WL Li and HJ Gibeling. Determination of the mutual radiation resistances of a rectangular plate and their impact on the radiated sound power. *Journal of Sound and Vibration*, 229(5):1213–1233, 2000.

[7] Dmitrii N Maksimov, Almas F Sadreev, Alina A Lyapina, and Artem S Pilipchuk. Coupled mode theory for acoustic resonators. *Wave Motion*, 56:52–66, 2015.

[8] Jacek Okołowicz, Marek Płoszajczak, and Ingrid Rotter. Dynamics of quantum systems embedded in a continuum. *Physics Reports*, 374(4):271–383, 2003.

[9] Shuping Wang, Jiancheng Tao, and Xiaojun Qiu. Performance of a planar virtual sound barrier at the baffled opening of a rectangular cavity. *The Journal of the Acoustical Society of America*, 138(5):2836–2847, 2015.

[10] Lei Xiong, Wenping Bi, and Yves Aurégan. Fano resonance scatterings in waveguides with impedance boundary conditions. *The Journal of the Acoustical Society of America*, 139(2):764–772, 2016.

[11] Cheng Yang, Jie Pan, and Li Cheng. A mechanism study of sound wave-trapping barriers. *The Journal of the Acoustical Society of America*, 134(3):1960–1969, 2013.